01 Oct 2005

Evaluation of Microwave Reflection Properties of Cyclically Soaked Mortar Based on a Semiempirical Electromagnetic Model

Shanup Peer

K. E. Kurtis

R. Zoughi
Missouri University of Science and Technology, zoughi@mst.edu

Recommended Citation

S. Peer et al., "Evaluation of Microwave Reflection Properties of Cyclically Soaked Mortar Based on a Semiempirical Electromagnetic Model," *IEEE Transactions on Instrumentation and Measurement*, vol. 54, no. 5, pp. 2049-2060, Institute of Electrical and Electronics Engineers (IEEE), Oct 2005.
The definitive version is available at https://doi.org/10.1109/TIM.2005.853221

Evaluation of Microwave Reflection Properties of Cyclically Soaked Mortar Based on a Semiempirical Electromagnetic Model

Shanup Peer, Kimberly E. Kurtis, and Reza Zoughi, *Senior Member, IEEE*

***Abstract*—Detection of chloride ingress and evaluation of its distribution and temporal movement in reinforced concrete structures is an important practical issue. Steel reinforcing bars embedded in good quality concrete are normally protected from corrosion. However, the presence of a sufficient concentration of free chloride ions in the region of the reinforcing steel can initiate the process of corrosion. Therefore, it is important to be able to detect ingress of chloride ions and their distribution in cement-based materials. Moreover, it is important to obtain this information nondestructively. In recent years, near-field microwave nondestructive evaluation methods, using open-ended rectangular waveguide probes, have proven effective for evaluating many important properties of cement-based materials, including the detection of salt, added to the mixing water and when entering these materials through exposure to salt solution. Additionally, successful electromagnetic modeling of the interaction of microwave signals with moist cement-based materials has provided the necessary insight for evaluating the distribution and movement of moisture within these materials, leading to the current study involving ingress of sodium chloride solution. To this end, a mortar cube was subjected to cycles of wetting in a sodium chloride bath with a salinity of 2.8%, followed by episodes of drying. Subsequently, the microwave reflection properties of the cube were measured at 3 and 10 GHz using open-ended rectangular waveguides for several cycles, each lasting about 35 days. A semiempirical electromagnetic model, representing the cube as a stratified structure with a nonuniform dielectric property profile, was then developed to simulate the measured reflection properties. The simulated and the measured results at both frequencies and for all cycles were in good agreement. Subsequently, the effect of ingress of salt solution in terms of the temporal distribution of moisture along with the dissolved salt (i.e., pore solution) within the cube for every cycle was also estimated. This paper presents a brief description of the measurement approach and a detailed description of the model and its results.**

***Index Terms*—Chloride, concrete, corrosion, microwaves, nondestructive testing.**

I. Introduction

CHLORIDE ingress is an important cause of steel corrosion in reinforced concrete structures in North America. Corrosion of the reinforcing steel is implicated as a cause of damage to the majority of the 226 000 reinforced concrete bridges described by the Federal Highway Administration (FHWA) as deficient [1], [2]. In 1991, the U.S. Department of Transportation estimated rehabilitation costs for these damaged bridges at $90.9 billion [2]. In Canada, an estimated CAD$200 million (or USD$140 million) is spent *annually* to repair some 600 parking structures experiencing corrosion [3]. Designing concrete structures based upon strength criteria rather than durability criteria, the growing use of chloride-containing deicing salts, and extension of construction activity to increasingly aggressive environments are some of the factors that have led to the increase in concrete structures experiencing reinforcement corrosion in recent decades.

Due to its inherent alkalinity and impermeability, good quality concrete adequately protects reinforcing steel from corrosion. When steel is encased in concrete, a protective passive film forms on the steel surface due to the high pH of the concrete. This film largely protects the steel from corrosion. However, the presence of a sufficient concentration of chloride ions near the steel in reinforced concrete can compromise the passivation of the steel. Subsequently, when moisture and oxygen are present in the concrete, corrosion of reinforcing steel bars can occur [4], [5]. Chloride ions can be introduced into the concrete during its manufacture when seawater or water with a high chloride concentration is used, when chloride-contaminated coarse or fine aggregates are used, or when chloride-containing admixtures are used. However, usually the corrosion of reinforcing steel is caused by the ingress of chloride ions present in the surrounding environment of a concrete structure. Deicing salts, seawater, and chloride-contaminated soils are the primary sources of external chloride.

Limits on the amount of chloride in reinforced concrete are set in two ways: the amount of water-soluble chloride ions, and the total chloride-ion content. The two values are substantially different from one another because the water-soluble chloride is only a part of the total chloride content. The "free" chloride ions, those dissolved in the pore solution, participate in the corrosion process [4]. On drying, free chlorides form products that can be dissolved upon rewetting.

Standard test procedures for the water-soluble chloride-ion content of hardened concrete are described in [6] and [7]. These tests are destructive in nature and are performed in a laboratory on concrete that has hardened for 28 to 42 days. Another measure of chloride content in concrete, the total amount of chloride, can be found through procedures outlined in the American Society for Testing and Materials (ASTM) and the American Association of State Highway and Transportation Officials (AASHTO) [8], [9]. Both of these standards require that a core

Manuscript received September 16, 2003; revised November 9, 2004. This work was supported by The National Science Foundation under Grant NSF CMS-0196158. Any opinion, findings, and conclusions or recommendations expressed in this material are those of the authors and do not necessarily reflect the views of the National Science Foundation.

S. Peer and R. Zoughi are with the Applied Microwave Nondestructive Testing Laboratory (AMNTL), Electrical and Computer Engineering Department, University of Missouri-Rolla, Rolla, MO 65409 USA.

K. E. Kurtis is with the School of Civil and Environmental Engineering, Georgia Institute of Technology, Atlanta, GA 30332 USA.

Digital Object Identifier 10.1109/TIM.2005.853221

of concrete be ground into a powder and be tested in a laboratory. Once the sample is obtained, it is crushed and tested by the procedures outlined in [8]–[14].

Development of a reliable test method for *in-situ* measurement of the chloride ion penetration in in-service concrete would be invaluable to the concrete and construction industries. From an economic standpoint, accurate measurements of the concentration of chlorides and penetration depth in concrete structures would allow agencies to more effectively allocate funding for repair of those structures with the most critical needs and to identify those concrete mixtures with superior field performance. The broader goal of this work, then, is to assess the potential application of a microwave method for *in-situ* monitoring of chloride ingress in cement-based materials.

II. Background

Near-field microwave nondestructive testing and evaluation (NDT&E) techniques, using open-ended rectangular waveguide probes and monopole antennas, have been used to interrogate a wide variety of cement-based materials for their important physical and structural properties. They include the following: evaluation of water-to-cement ratio (w/c) and compressive strength of hardened cement paste [15], [16], evaluation of fresh concrete w/c [17], evaluation of porosity and sand-to-cement ratio (s/c) in mortar [18], [19], evaluation of mortar permittivity using a combined microwave near-field and modulated scattering technique [20], evaluation of coarse aggregate-to-cement ratio (ca/c), monitoring of cure-state and material properties of concrete [21]–[24], detection of grout in masonry bricks [25], and detection of de-bonding between hardened cement paste and fiber reinforced polymer (FRP) composites [26], [27].

In recent years near-field microwave NDT techniques have also been extensively used in evaluating chloride contamination in cement-based materials. It has been shown that the addition of salt to the mixing water of mortar can be easily evaluated using these techniques [28]. It has also been shown that the influence of cyclical chloride ingress in mortar exposed to sodium chloride solution can also be evaluated using these techniques [29]–[33]. This paper briefly presents the results of an extensive investigation in which a mortar cube is cyclically exposed to sodium chloride solution. The focus of this investigation is the development of a semiempirical electromagnetic model simulating the reflection properties of the soaked mortar cube, based on the temporal dielectric properties of the cube as a function of the cube depth. The outcome of such a model would then provide useful information regarding the volumetric distribution of dissolved salt (i.e., in the pore solution) as influenced by the ingress of salt solution.

III. Experimental Approach

Two mortar cubes of dimension $200 \times 200 \times 200$ mm ($8 \times 8 \times 8$ in), having a w/c of 0.50 and a s/c of 2.5, were produced using tap water and commercially available portland cement Type I/II [34]. The cubes were then placed in a hydration room for 24 h and subsequently left at room temperature and low humidity for another ten months. One of the mortar cubes was then submerged to within $\sim$6 mm ($\sim$1/4 in) of its top surface in sodium chloride solution having 2.8% salinity,

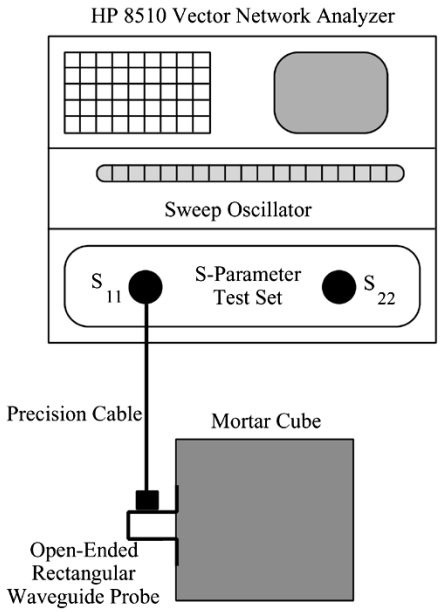

Fig. 1. Experimental apparatus.

while soaking for 24 h. The cube was then removed from the bath and left in ambient conditions for 24 h, in order for the excess solution on the surface of the cube to evaporate. The other cube was not soaked and left in ambient conditions to serve as the reference cube.

Subsequently, using open-ended rectangular waveguide probes, in conjunction with an HP8510 vector network analyzer, the daily reflection properties of the soaked and the reference cubes were measured at two different frequency bands, namely S-band (2.6–3.95 GHz) and X-band (8.2–12.4 GHz), as shown in Fig. 1. To obtain an average value of the reflection properties, 16 measurements were performed on the cube sides (four per side) at S-band, while 36 measurements (nine per side) were made at X-band. This procedure was followed for three such soaking and drying cycles, each of which lasting approximately 35 days. Concurrently, the masses of the cubes were also monitored on a daily basis, and this information was subsequently incorporated into the electromagnetic model as the only physical data. The measured results are shown, and the modeling analyses are performed for two specific frequencies of 3 GHz (S-band) and 10 GHz (X-band), representing each frequency band.

IV. Experimental Results

A. Influence of Soaking and Drying

Prior to soaking in salt solution, the mortar cube is primarily composed of cement hydration products, sand, residual unhydrated cement, intrinsic pore solution, and air (pores and cracks). However, once the cube is soaked, salt solution ingresses into the cube, filling the pores and cracks and mixing with the preexisting pore solution. Thus, the pore solution existing within the cube after exposure to the salt solution can be considered as a combination of the intrinsic pore solution and the salt solution that has ingressed into the cube during the soaking period. Further references to pore solution, unless explicitly stated, will refer to the mixing of external salt solution with intrinsic pore solution, rather than the intrinsic

pore solution prior to exposure. The composition of the pore solution, however, may vary with location within the cube and time of exposure to salt solution.

Once removed from the bath and exposed to the ambient conditions, the moisture in the cube begins to evaporate from its near surface regions, while some of the pore solution is drawn toward the cube core through the process of capillary draw, and possibly by diffusion. As the moisture evaporates, the pore solution reaches saturation concentrations for various compounds, and products likely including salt crystals precipitate out in the preexisting pores and cracks. In addition, some of the intruding chloride ions interact with calcium aluminate phases and other phases, thus becoming bound. In the context of this investigation, the products that precipitate from the pore solution and the newly formed bound chloride products are collectively referred to as "solid products."

Thus, the mortar cube while in solution can be represented as a multiphase dielectric mixture, where the host material comprises of hardened cement paste (containing both hydration products and a relatively small amount of residual unhydrated cement) and sand while the pore solution and air (pores and cracks) constitute the inclusions. However, once removed from the solution and exposed to ambient conditions, the gradual appearance of newly formed solid products within the cube can then be considered in the multiphase mixture as an additional inclusion phase. In addition, the distribution and composition of the pore solution will change. All of the above-mentioned factors contribute to variations in the temporal distribution as well as volumetric content of the various inclusions present within the cube during a given cycle. Consequently, the temporal microwave reflection properties of the cube vary during a given cycle as well.

B. Discussion of Experimental Results

This paper describes a model based upon experiments performed on a mortar cube subjected to wet/dry cycling in salt solution. The detailed results of this experiment have been published elsewhere and will not be repeated here [34]. However, it is important to mention some of the more important aspects of the results since they become the foundation for modeling the temporal reflection properties of the cube, and the determination of the temporal distribution of pore solution (due to cyclical exposure to salt solution) within it.

Fig. 2 shows the daily measured magnitude and phase of reflection coefficient (calibrated and measured at the aperture of the waveguide probe) for the soaked and the reference cubes at 3 GHz, respectively, for three soaking and drying cycles. It is observed that for the soaked cube and for each cycle, $|\Gamma|$ increases significantly from its presoaked value (i.e., day zero in cycle 1) to the value measured at the first day of the measurement cycle (i.e., day two in cycle 1), indicating the ingress of salt solution into the cube, as expected. During the subsequent days, $|\Gamma|$ gradually decreases, primarily indicating the evaporation of water from the cube. The gradual increase in the measured phase of reflection coefficient is also indicative of the same phenomena [34], [35]. However, one important aspect regarding the reflection properties is that a distinct dip occurs in the phase of reflection coefficient during the first few days of the cycle after which it gradually increases as a function of days beyond this point. The gradual increase (after the first few days) could be primarily attributed to the evaporation of water. However, the dip

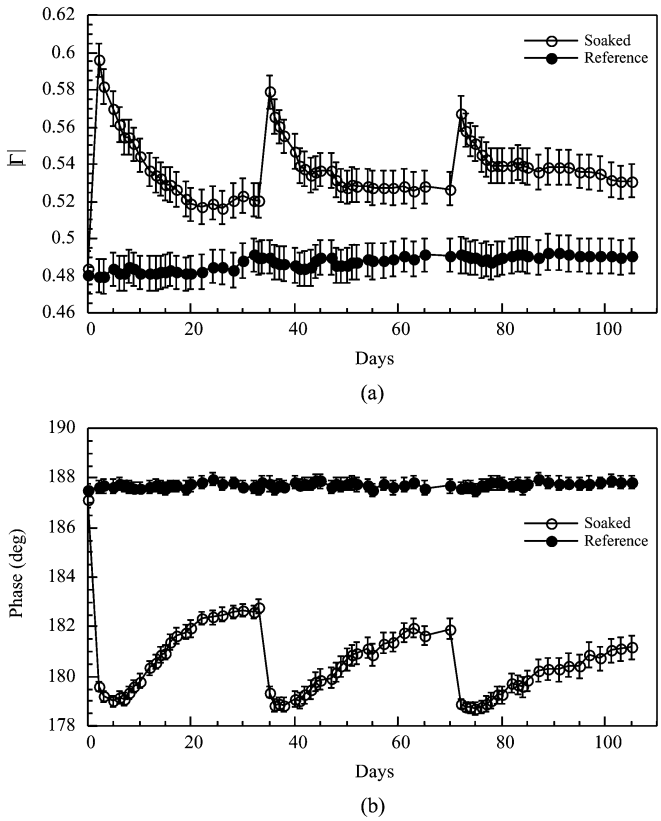

Fig. 2. (a) Magnitude and (b) phase of reflection coefficient for the three cycles at 3 GHz for the soaked and the reference cube.

is believed to be indicative of an important phenomenon that is occurring within the cube. It is believed that this dip is caused by the temporal variations in the pore solution distribution within the cube, as will be described in Section V. The reflection properties of the reference cube remain fairly constant throughout the entire period, as expected.

In addition to the reflection property measurements, the mass of the cubes were also measured on a daily basis. Fig. 3 shows the mass relative to the presoaked mass (i.e., additional mass) of the cubes as a function of days, indicating the total mass gain (i.e., due to soaking) and loss (i.e., due to evaporation) with time. It is important to note that the mass of the soaked cube at the end of a cycle is greater than its mass at the end of each previous cycle, indicating that some additional pore solution and some additional solids remain in the cube at the end of each cycle. These are important observations that must be considered when developing the electromagnetic model simulating the reflection properties of the cube. As a result of the variation in the temporal moisture content within the cube, the signal penetration into the cube also varies (i.e., more signal penetration in the latter days of the cycle since the cube is relatively drier at this time). Therefore, to obtain more comprehensive information about the temporal nature of the pore solution distribution within the cube, measurements were conducted at two frequency bands, namely; S-band (2.6–3.95 GHz) and X-band (8.2–12.4 GHz). Frequencies at the latter band provide information about the near-surface properties of the cube while the former band provides information about the deeper regions of the cube.

The variation in the reflection properties of the soaked cube as a function of days is a clear indication of the fact that the dielectric properties of the cube are varying as a function of

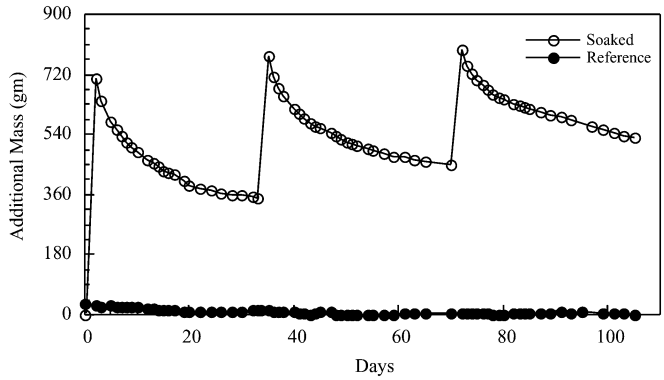

Fig. 3. Additional mass for the soaked and the reference cube.

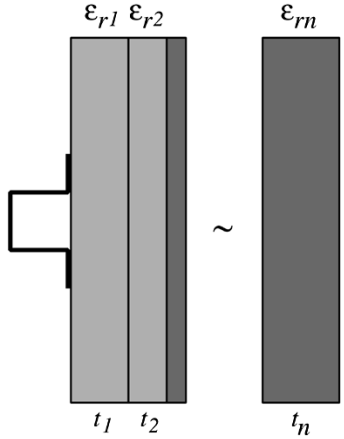

Fig. 4. Schematic of an open-ended rectangular waveguide probes interacting with a multilayered structure used in the modeling process.

days, and as will be shown later, also as a function of depth into the cube. Thus, the objective of this investigation is to develop a semiempirical electromagnetic model simulating the measured temporal reflection properties of the soaked cube for each cycle and for the two distinct frequencies. The outcome of this model would then yield useful information regarding the temporal pore solution distribution within the cube. The first prerequisite for the development of such a model is the conceptualization of the various phenomena that might be occurring within the cube and how they influence the dielectric properties as a function of time and depth into the cube.

V. Modeling Approach and Considerations

The macroscopic behavior of dielectric materials is described by a parameter known as the dielectric constant (dielectric properties). In general, this is a complex parameter whose real part (absolute permittivity) indicates the ability of the material to be polarized or store microwave energy, while its imaginary part (absolute loss factor) indicates the ability of the material to absorb microwave energy. When referenced to the permittivity of free-space, these parameters are referred to as the relative permittivity and loss factor, respectively. The calibrated effective reflection coefficient of the cube, measured at the waveguide aperture is a function of the effective dielectric properties of the cube. The effective dielectric properties of the cube are correspondingly dependent on the following:

1) the dielectric properties of the host material (mortar in this case);
2) the dielectric properties of the various inclusions present within the cube at any given day, which varies as a function of depth into the cube;
3) the volume fractions of the host material and the various inclusions in the cube at any given day (the latter is also a function of depth into the cube) [36], [37].

As mentioned earlier, the average reflection properties of the soaked cube (hereafter referred to as the cube) were measured at two different frequency bands. Consequently, the resulting average values for $|\Gamma|$ and phase, the spatial reflection properties, and hence the material properties, of the cube across its sides is now considered to be uniform with the variations in the properties only existing along the distance into the cube [35]. Although this variation in the dielectric properties is continuous as a function of distance from the surface, for modeling purposes, the mortar cube can be analyzed as a collection of many discrete layers. In this way, the mortar cube can be modeled as a collection of discrete layers (into the cube) each with a thickness and effective dielectric properties. Subsequently, a multilayered formulation that gives the magnitude and phase of reflection coefficient, measured by an open-ended rectangular waveguide probe, for a stratified dielectric material at a specified frequency; number of layers n and thickness t_n, and the dielectric properties of each layer $\varepsilon_{\rm rn}$ was utilized for obtaining the temporal reflection properties of the cube [38], as shown in Fig. 4.

In a previous investigation, the microwave reflection properties of a similar mortar cube that was soaked in distilled water was successfully modeled [35]. The outcome of the modeling process resulted in evaluating and obtaining the temporal water distribution in the cube for the same three soaking and drying cycles. This extensive modeling effort provided the necessary insight into the dynamics of temporal mass transport within the water-soaked cube as it relates to properly simulating the microwave reflection properties of the cube at 3 and 10 GHz. Therefore, the electromagnetic modeling of the reflection properties of the cube soaked in salt solution, which is of interest here, is based on this previous modeling effort. However, important influences caused by the presence of salt, in its ionic (dissolved in the pore solution) and solid forms, must be properly accounted for so that the microwave reflection properties of the cube are closely simulated.

The modeling process for the water-soaked cube revealed certain important features about the temporal water distribution within the cube. One of the primary outcomes of the investigation was the general behavior of the water distribution function. The resulting water distribution within the cube (i.e., as a function of depth into the cube) showed the following:

1) minimal water content near the surface (due to evaporation);
2) gradual increase in water content until a maximum value is reached at a certain thickness;
3) decrease in water content from this point on [35].

This was represented by a Rayleigh-like distribution possessing the aforementioned characteristics. Consequently, the general equation for the water distribution was obtained which is used in the present study for the pore solution distribution, denoted by $\mathrm{PSD}(t)$ and expressed by

$$\mathrm{PSD}(t) = k_4 \left[\frac{t}{k_1}\right]^{k_2} e^{\left[-k_3\left(\frac{t}{k_1}\right)^{k_2}\right]} \,(\mathrm{gm/mm}) \qquad (1)$$

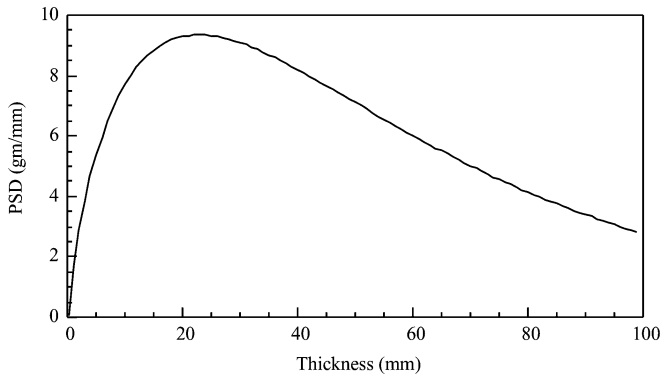

Fig. 5. Rayleigh-like distribution function simulating the pore solution distribution in the cube.

where t is the thickness, which varies from the surface of the cube to its center (i.e., 0 to 100 mm), k_1, k_2, k_3 are empirical parameters and k_4 is proportional to the maximum value (amplitude) of the distribution function for each day. Fig. 5 shows the general shape of this distribution function as a function of thickness into the cube. One additional and important piece of information was also obtained from modeling of the water-soaked cube. It was determined that to properly simulate the shape of the phase of reflection coefficient during the first few days of drying (i.e., where it exhibits a flattened shape) the distance at which the peak of water distribution functions occurred could not remain fixed, and varied as a function of days, indicating the movement of water between the layers. To simulate this effect, the values of the empirical parameters k_1, k_2, k_3, and k_4 also changed as a function of days [35]. However, it should be noted that these empirical values would be different for the salt solution-soaked cube compared to the water-soaked cube as a result of the following:

1) presence of salt;
2) any additional phenomena due to the presence of salt;
3) the total mass of pore solution present in the cube (which would be different from that of the water-soaked cube) on any given day.

The daily mass of the soaked cube is used as the only physical input data to the model and serves as the starting point to this modeling process. This mass is first divided by five to obtain an adjusted mass, which represents the change in mass of pore solution (i.e., due to the ingress of salt solution) that influences the microwave signal, and hence the reflection properties for each day [35]. This is done to account for the nonuniform contribution, from each side of the cube, to the additional mass of pore solution present in the cube [35]. The integral of the distribution function, characterized by a combination of specific values for k_1, k_2, k_3, and k_4 for any given day, must then match this adjusted mass for each day.

As water evaporates from the layers, it results in 1) an increase in the ionic concentration of the remaining pore solution and 2) the precipitation of salt crystals and the formation of bound salt in each of the layers, which causes a corresponding decrease in the dissolved salt and, hence, the ionic concentration of the pore solution. To account for both these effects, it would therefore be useful to know when (or at what concentration) salt crystals and other solid products would begin to precipitate out of the pore solution. For example, a salinity of around 35% can be achieved for NaCl in pure water. However, in pore solution, the presence of other ions (e.g., OH^-, Ca^{++}, K^+, Na^+, and Mg^{++}, among others) decreases the solubility of the NaCl. Therefore, it is likely that the concentration of Na^+ and Cl^- in solution, prior to crystallization, may not reach the concentration predicted by its solubility product. In addition, the presence of these other ionic species in the pore solution makes it likely that solid products other than NaCl will be formed. Each of these will precipitate out then when their own solubility limit in this complex pore solution has been reached. Consequently, the pore solution composition can vary considerably, and it is difficult to predict the maximum concentration of Na^+ and Cl^- in the pore solution when the precipitation of chloride-containing solid phases occurs. In the absence of such experimentally derived data, it is useful to also extract this information from this semiempirical electromagnetic model which describes the change in the measured microwave reflection properties of the mortar cube exposed to salt solution. It was observed that the results of the model and the measured reflection properties (magnitude and phase and for both frequencies) matched quite well when the ionic concentration was fixed to a certain level which in terms of equivalent salinity (ratio of mass of dissolved salts to mass of solution) corresponded to a value of around 5%. A detailed discussion of the choice of this limit, henceforth referred to as "threshold value," is provided in Section VII.

For the purpose of modeling, the initial condition for the pore solution distribution (due to the ingress of salt solution) is considered to exist within the cube immediately after it is taken out of the salt solution bath, and once left in the ambient conditions, this initial condition changes. In order to be able to simulate the reflection properties accurately, it then becomes imperative to consider the effect of the formation of solid products as well as the total ionic concentration (of each layer) while calculating the dielectric properties of each layer. To account for both these factors, the nominal "maximum pore solution content" (volumetric) in each layer has to be estimated. It is obvious that the maximum pore solution content in any layer would have existed when it was initially taken out of the saltwater bath (i.e., day one). For this purpose, the day one pore solution distribution (the day when the cube was left in the ambient conditions, and no microwave reflection measurements were conducted) was extrapolated from the day two (first day of microwave measurements) distribution.

The formation of solid products causes a reduction in the ionic concentration of the remaining pore solution. Conversely, if the nominal ionic concentration of the pore solution in any layer is not allowed to increase beyond a certain threshold value, the effect of solid product formation is then implicitly built into the model. In the present model, the ionic concentration of the pore solution in each layer for every day was first compared to the threshold value. If the ionic concentration of any of the layers for any day increases beyond this threshold value, then the ionic concentration of that particular layer for that particular day was set to the threshold value.

Finally and subsequent to accounting for all of the abovementioned issues, the modeling process was initiated. The following is the step-by-step modeling procedure.

1) The daily mass of the cube is subtracted from its presoaked value to obtain the uptake of salt solution. This value is then divided by five, as mentioned earlier to obtain the adjusted mass and is denoted by m [35].

2) Setting $k_4 = 1$, the integral of the pore solution distribution (i.e., total pore solution due to ingress of salt solution) is calculated over a cube thickness of 100 mm (i.e., halfway through the cube), namely

$$\text{TPS} = \int_{t=0}^{t=100} \text{PSD}(t)\, dt \text{ (gm)}. \tag{2}$$

The signal penetration into the cube is expected not to exceed more than halfway in the cube, and the moisture uptake is also not expected to exceed this point. This fact has been experimentally verified [34]. It is important to mention here that by subtracting the daily mass of the cube from the presoaked mass, the contribution of intrinsic pore solution no longer needs to be explicitly considered in the model, since this contribution is already included in the dielectric properties of presoaked mortar cube. Consequently, PSD(t) represents the pore solution distribution due to salt solution ingress.

3) k_4 is now set to the ratio of m and TPS (i.e., m/TPS).
4) The cube is then discretized into 100 layers, each having a thickness of 1 mm. It is important to note that this model provides for any arbitrary layer thickness, and hence it is able to provide fine pore solution distribution resolution.
5) With the updated value of k_4, the integral of the total pore solution is found for every 1 mm layer of the cube, namely

$$\text{TPS}(t_1) = \int_{t_1}^{t_1+1} \text{PSD}(t)\, dt \text{ (gm)}. \tag{3}$$

6) The mass of salt uptake in each layer is obtained from the extrapolated pore solution distribution at day zero, and the mass of solution is obtained from step 5). The ionic concentration of the pore solution present in each layer was then found from its "equivalent salinity" (i.e., ratio of mass of the salt to the mass of the solution).
7) A formulation that was developed for determining the dielectric properties of brine having varying salinity based on its conductivity was then utilized to determine the dielectric properties of the pore solution in each layer for each day [36]. As the ionic concentration of the pore solution increases (as a function of days), it causes a significant increase in the conductivity of the mortar cube. Thus, any over-estimation of the pore solution content in any of the layers results in incorrect incorporation of the dielectric properties of the individual layers in the model, and hence the simulated microwave reflection properties will not match its measured counterparts. It is for this purpose that the effects of solid product formation (resulting from salt solution ingress), which would subsequently cause a decrease in the overall ionic concentration of the pore solution within the cube, has been considered in the model. To illustrate the effect of setting the equivalent salinity of the pore solution to a maximum of 5%, the dielectric properties of the pore solution for a particular thickness (layer 2) of the cube for several days of the cycle were calculated, as shown in Table I.

TABLE I
COMPARISON OF THE DIELECTRIC PROPERTIES OF A LAYER AS A FUNCTION OF DAYS WITH AND WITHOUT THE CONSIDERATION OF A MAXIMUM SALINITY LEVEL

Days	Calculated equivalent Salinity (%)	Dielectric Properties	Equivalent salinity with a 5% Threshold	Dielectric Properties
0	2.9	68 – j37	2.9	68 – j37
10	7.1	58 – j65	5.0	63 – j51
18	9.4	53 – j79	5.0	63 – j51
27	12.4	47 – j95	5.0	63 – j51

8) If the ionic concentration of the pore solution [from Step 6)] in any of the layers is greater than the threshold value, corresponding to an equivalent salinity of 5%, then the ionic concentration of the pore solution in that particular layer is set to the threshold value. The remaining mass of salt that would have contributed to a higher ionic concentration than the threshold value is then calculated. This remaining mass of salt in the layer then exists as solid products. Furthermore, the dielectric properties of the newly formed solid products (i.e., chloroaluminates or other products, including salt crystals) are similar since they are expected to be in the family of low-loss, low-permittivity materials. In that case, it is believed that treating all solid products as salt crystals in the model would have negligible effect on the simulated reflection properties. The dielectric properties and volume fraction of the excess salt is then approximated as salt crystals and represented by ε_{rs} and f_s and is included in the dielectric mixing formula to determine the dielectric properties of each layer. The dielectric properties of various salts including NaCl (used in this investigation) had also been measured extensively in previous investigations [30], [31].
9) A dielectric mixing formula was then used to determine the effective dielectric properties of each layer. Although there are numerous dielectric mixing formulae available that could be used to evaluate the effective dielectric properties of a multiphase mixture, most of these render similar results when the inclusion volume fractions are relatively small (i.e., air, pore solution, salt) [36], [37], [39]. The following dielectric mixing formula was then used to calculate the effective dielectric properties $\varepsilon_{\text{reff}}$ of every 1-mm-thick layer of the mortar cube

$$\varepsilon_{\text{reff}} = \varepsilon_{\text{rps}} f_{\text{ps}} + \varepsilon_{\text{rm}} f_m + \varepsilon_{\text{rs}} f_s + f_a \tag{4}$$

where

- ε_{rps} complex relative dielectric property of pore solution. This quantity varies as a function of ionic concentration of the pore solution,
- ε complex relative dielectric property of mortar,
- ε_{rs} complex relative dielectric property of solid inclusion. This quantity represents the formation of solid products resulting from the salt solution ingress,
- f_{ps}, f_m, f_s, and f_a are the volume fractions of pore solution, mortar, solid inclusion, and air respectively, in each 1-mm-thick layer (i.e.,

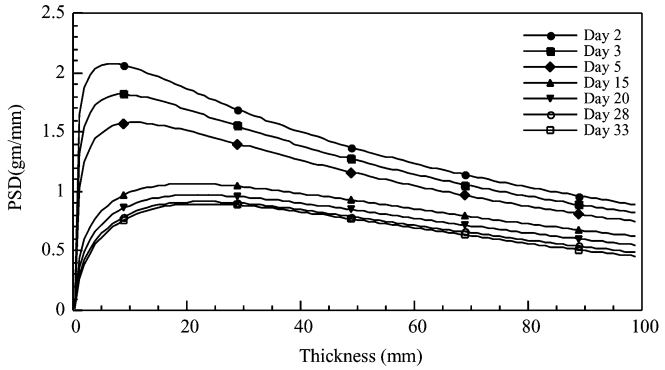

Fig. 6. Pore solution distribution in the cube for cycle 1.

$f_{sw} + f_s + f_a = 1 - f_m$). The dielectric properties of mortar has been measured previously [18], [19], [34]. It is important to note that all of the quantities in (4), except $\varepsilon_{\rm rm}, \varepsilon_{\rm rs}$, and f_m vary as function of days and depth into the cube (i.e., the location of the respective layer in the discretized cube).

10) Once the dielectric properties of each of the 100 layers were obtained, the multilayered formulation was evoked to simulate the reflection properties of the cube at the waveguide aperture [38].
11) The values of k_1, k_2, and k_3 were subsequently and rigorously adjusted based on a comparison between the measured and the corresponding simulation results for $|\Gamma|$ and phase at 3 and 10 GHz.
12) The above-mentioned procedure was carried out for each day of each cycle. The final values of k_1, k_2, and k_3 for each day were then used to determine the pore solution distribution in the cube. It is important to note that this "distribution" will capture changes in ionic concentration as well as volume of the pore solution, resulting from salt solution ingress.

VI. Results

A. Cycle 1

Fig. 6 shows the pore solution distribution, for several days of cycle 1, obtained from this modeling process. The results show several important phenomena. The first measurement corresponds to day two (i.e., 24 h after removing the cube from the salt solution bath). At this time, it is expected that any moisture immediately at the surface has evaporated. The curves representing the pore solution distributions clearly indicate this phenomenon. Additionally, they also show that the pore solution distribution rapidly increases as a function of distance into the cube. A comparison of the distribution curves shows that as the days progress there is a change in 1) the general shape of the distributions and 2) the position at which the peak of pore solution distribution occurs. It is also observed that as the days progress, the rate at which the peak of the pore solution content moves toward the core of the cube decreases, and the change in the shape of the distributions becomes less pronounced. This may be attributed to a state of equilibrium being reached between the evaporation of moisture from each layer and the movement of pore solution (due to variation in concentration) between the layers.

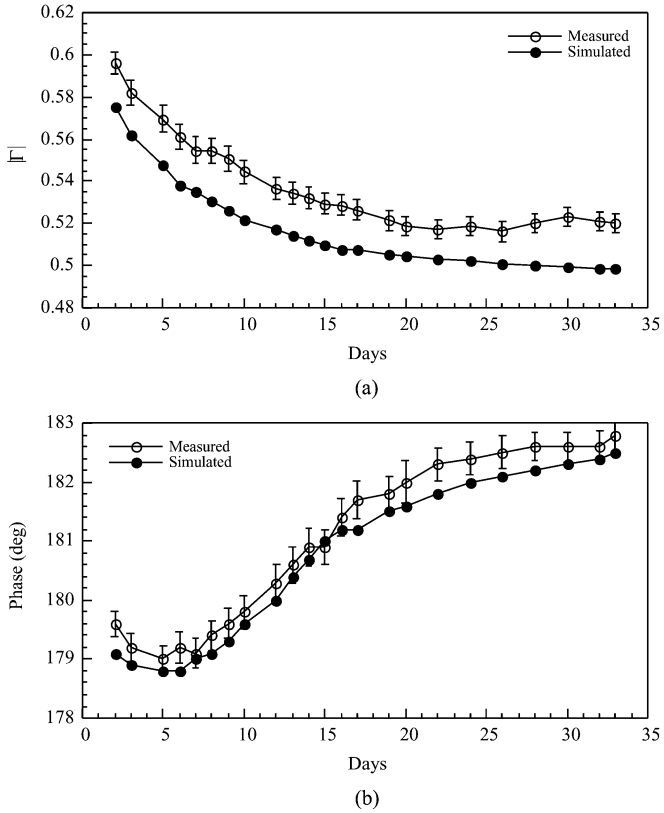

Fig. 7. Comparison of the measured and simulated reflection coefficient of the cube at 3 GHz and for cycle 1 (a) magnitude and (b) phase.

Once the empirical factors k_1, k_2, and k_3 were determined, the effective dielectric properties of each of the layers were calculated and then fed into the multilayered formulation to simulate the microwave reflection properties, as described in the modeling section [38]. Figs. 7 and 8 show the simulated $|\Gamma|$ and phase of reflection coefficient at S-band (3 GHz) and X-band (10 GHz), respectively. Clearly, good agreement is obtained between the simulated and measured results for both frequencies. Fig. 7(b) shows the comparison between the simulated and measured phase of reflection coefficient at 3 GHz. One important behavior of the phase of reflection coefficient is that it exhibits a distinct and relatively wide dip during the first few drying days. The simulation results, based on the obtained pore solution distributions as shown in Fig. 6, also replicate this distinct shape. During the simulation of the reflection properties of the water-soaked cube, it became evident that to properly simulate this distinct dip, the peak of the water distribution had to be carefully moved into the cube as a function of days [35]. This behavior was also incorporated in this model, and as expected, the distinct dip in the phase was correctly simulated. A closer inspection of the pore solution distributions shown in Fig. 6 indicates this phenomenon.

B. Cycle 2

After obtaining satisfactory results for cycle 1, the model was applied to simulate the reflection properties for cycles 2 and 3. The step-by step modeling process adopted for cycle 1 was again followed for these two cycles with a notable exception. When the cube is soaked again, it absorbs the salt solution with a salinity of 2.8% (salinity of the soaking solution). However,

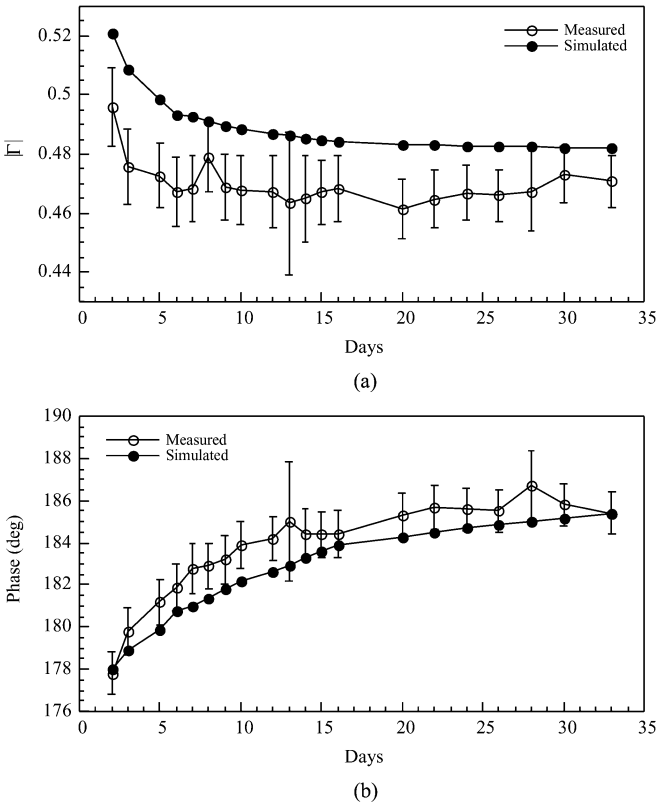

Fig. 8. Comparison of the measured and simulated reflection coefficient of the cube at 10 GHz and for cycle 1 (a) magnitude and (b) phase.

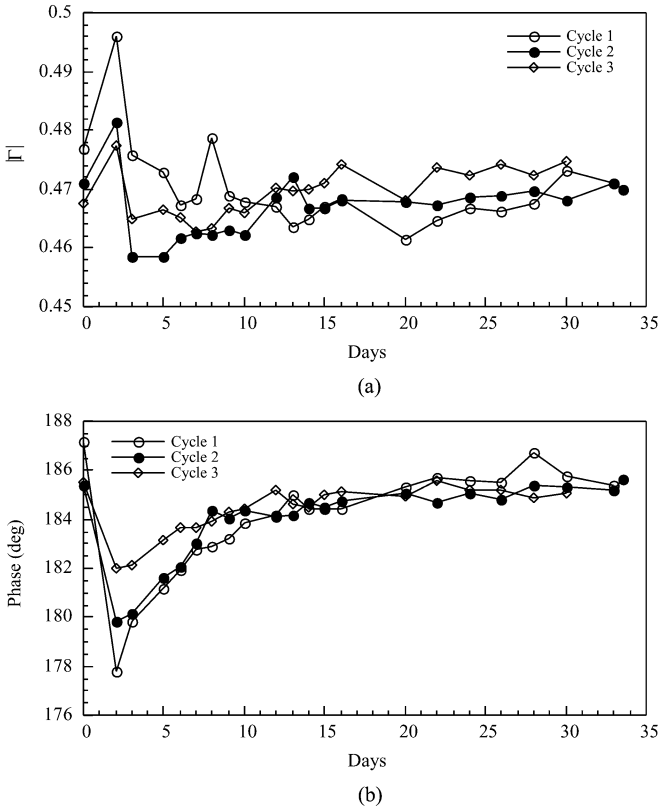

Fig. 9. Measured reflection coefficient of the cube at 10 GHz for all cycles (a) magnitude and (b) phase.

when this salt solution permeates into the cube, its ionic concentration immediately increases due to the influence of soluble solid products and the ions present in the pore solution resulting from the previous cycle. Subsequent to accounting for this behavior, the total mass of salt (i.e., the residual salt from cycle 1 and the newly ingressed salt from cycle 2) was then calculated and used to find the nominal ionic concentration of the pore solution in each layer as mentioned in the modeling process.

Subsequent to following the same modeling procedure as in cycle 1, the reflection properties at both frequency bands, especially the distinct dip in the phase of reflection coefficient at 3 GHz could not be accurately simulated. To understand the reason for this, a comparison between the measured reflection properties for each cycle at X-band was carried out. Fig. 9 shows the measured reflection properties for all three cycles at 10 GHz. As is evident from Fig. 9(a), for the first day of each cycle (i.e., day two in Fig. 9), $|\Gamma|$ gradually decreases while the phase of reflection coefficient [Fig. 9(b)] progressively increases as a function of cycles. Based on the effective depth of penetration of the microwave signal at this frequency, this behavior could be as a result of a decrease in the pore solution content in the near surface layers as a function of cycles. Subsequently, it became necessary to look into the material properties of the cube in more detail.

When the cube is soaked, the salt solution permeates into it through several processes such as diffusion, capillary draw, etc. [40]. These processes are primarily governed by the initial conditions prevailing within the cube at the time of soaking. In the case of cycle 1, the initial condition is a relatively dry mortar cube, whereas in the case of cycle 2, the initial condition is a mortar cube that has some residual pore solution as well as solid products left behind from cycle 1. Another factor that could contribute to variations in the conditions from cycle 1 to cycle 2 is the hygroscopic property of salt which causes it to retain water when other mineral phases in mortar may be experiencing drying. This property of salt may become more pronounced in cycle 2 due to the increasing amount of salt that is now present in the cubes (especially toward the surface) as a result of two factors:1) the residual salt left behind in the cube from cycle 1 and 2) the additional salt solution that has permeated into the cube during the second cycle. All of the above mentioned factors, therefore, contribute to the permeation and, hence, the distribution and variation of pore solution during the second cycle to be different from that of cycle 1.

With this in mind, to be able to match the simulation results to the measured reflection properties for cycle 2, it thus became necessary to move the peak of the pore solution distribution (for day two) further toward the core in comparison to that of day two of cycle 1, thereby reducing the pore solution content in the layers near the surface. Although this resulted in a better match between the simulated and measured results for X-band, it did not improve the S-band results significantly. To improve the S-band results, however, required that the peaks moved slightly toward the surface for the next few days *after* day two. Hence, to satisfy the requirements at both frequencies, the peak of the distribution curve for day two of cycle 2 was moved further toward the core with respect to that of day two of cycle 1. However, in contrast to the movement of the peak toward the core for subsequent days in cycle 1, the peak moved toward the surface for the next few days of cycle 2. Fig. 10 shows the resulting pore solution distribution for cycle 2. The resulting simulated reflection properties for cycle 2 at 3 GHz

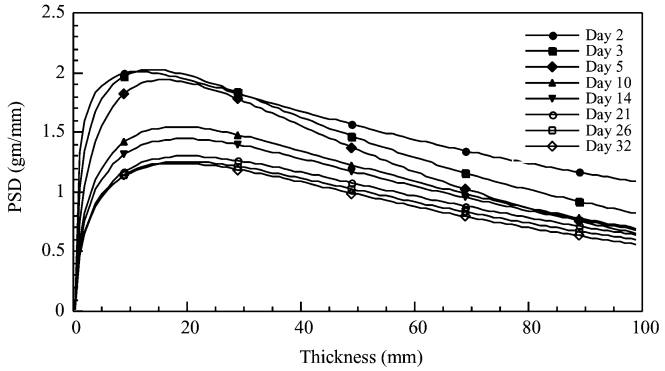

Fig. 10. Pore solution distribution in the cube for cycle 2.

are shown in Fig. 11. As expected, the results now show good agreement between the simulated and measured reflection properties. The results at 10 GHz for cycle 2 and at 3 and 10 GHz for cycle 3 also showed good agreement between the simulated and measured reflection properties [41]. These results have been omitted in the interest of brevity.

VII. Discussion

The simulation of the reflection properties of the salt solution-soaked cube was based on the choice of several parameters, which requires further discussion. When salt solution ingresses into the mortar cube, additional byproducts (such as Friedel's salt) may form by chemical interaction with existing hydration products and residual unhydrated cement. As stated previously, these products may be considered as additional inclusion phases. However, these additional inclusion phases can only be determined from a thorough investigation of the various chemical reactions that occur within the cube. Furthermore, it becomes necessary to determine how these additional products could be represented from an electromagnetic point of view (i.e., their effective dielectric properties). It would also be prudent to evaluate the sensitivity of the model to these parameters to justify their incorporation into and influence on the overall reflection properties. Although these additional inclusion phases have not been explicitly considered here, the model is versatile enough to account for them once their volume fraction is accurately determined.

As water evaporates from the cube, the ionic concentration of the remaining pore solution increases. The ionic concentration of the pore solution for every layer was calculated based on modeling the amount of dissolved salt and pore solution present in these layers for each day of each cycle [i.e., $\varepsilon_{\mathrm{rps}} f_{\mathrm{ps}}$. in (4)]. The effect of solid product formation (including products resulting in chloride binding) is considered by setting a threshold or maximum value that the ionic concentration of the pore solution in any of the layers can reach. The difference between the total salt ingress and the amount of Na^+ and Cl^- in the pore solution is then the amount of sodium and chloride that have formed solid products. The ionic concentration level is dependent on several factors such as the binding properties of mortar, moisture content, pore size, and cement composition, among others. It is important to note that these factors can also change as a function of time. The model was initially developed keeping this threshold value as the unknown parameter. Several iterations of the model were then carried out using different threshold

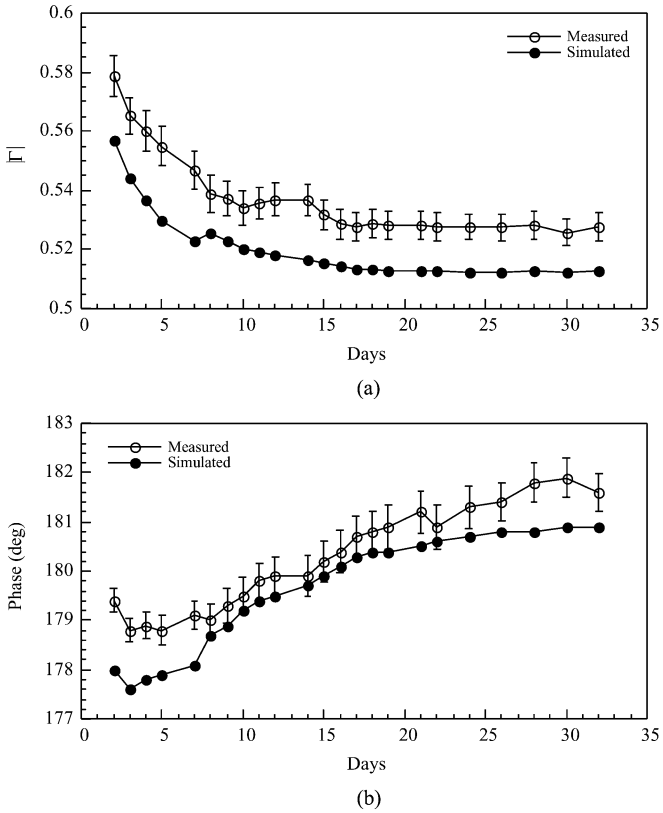

Fig. 11. Comparison of the measured and simulated reflection coefficient of the cube at 3 GHz and for cycle 2 (a) magnitude and (b) phase.

values. It is important to point out that the important issue regarding this investigation is the ability to simulate the reflection properties accurately by iteratively varying the temporal state of the cubes in terms of its dielectric properties. Considerable similarity (in both trend and value) between the measured and simulated reflection properties, if achieved, would then indicate that the temporal state of the cubes as represented in the model closely match those of the actual conditions.

Fig. 12(a), and (b) shows the simulation results of the microwave reflection properties at 3 GHz for different cases of threshold value in terms of maximum equivalent salinity level, for cycle 1. The results indicate that, while there is considerable similarity between the measured and all three simulated cases for the magnitude of reflection properties, only the 5% case shows similarity in both trend and value for the phase of reflection properties throughout the cycle. Consequently, the threshold of around 5%–6% was used for all the three cycles in the model. An interesting aspect however, is that, for the first few days of the cycle, all of the three cases in Fig. 12 results in the phase of reflection properties to be similar to that of the measured case. This is believed to be due to significant amounts of water remaining in the layers during these days, so that the ionic concentration does not reach the threshold value. With the passage of days, and after significant amount of water has evaporated from the layers, the ionic concentration in these layers tends to increase beyond the threshold value. In such a scenario, the threshold value tends to play a crucial role and significantly influences the calculated dielectric properties of each layer. Consequently, the dissimilarity in the phase of reflection properties between the 5% and 10%, 14% begins to increase for the final days of the cycle, as seen in Fig. 12(a), and (b). This

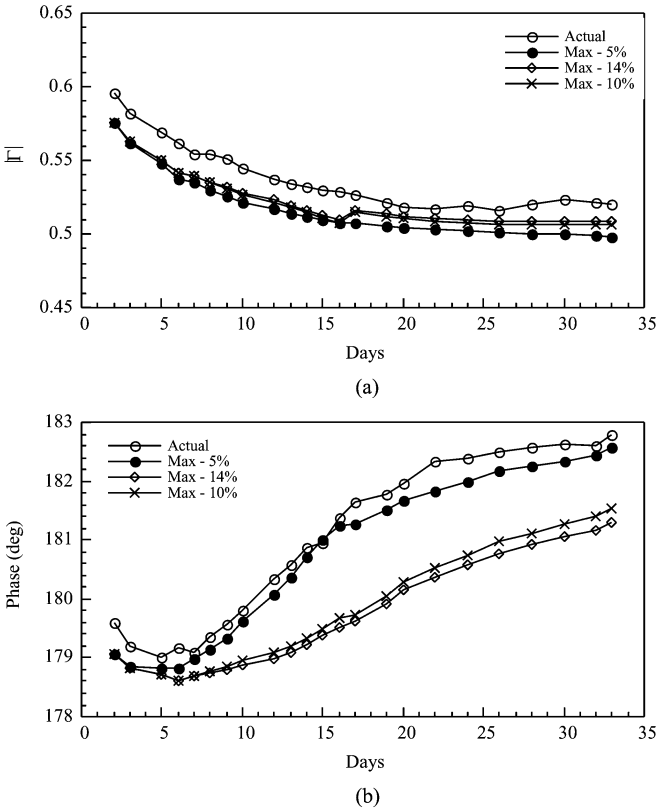

Fig. 12. Comparison of the measured and simulated reflection coefficient of the cube at 3 GHz and for cycle 1 (a) magnitude and (b) phase for three different threshold values.

threshold value, however, needs to be further investigated and could be represented in the model as a function rather than a constant with respect to cycles. Additionally, the relationship between the free, bound, and total amount of chloride can be incorporated in the model to represent the bound chlorides explicitly in the model. If this can be achieved, then the model would be able to assess the free salt profile as well as a profile of the bound chlorides as a function of days and cycles.

Finally, there is an issue regarding whether or not the pore solution distributions that were obtained from this model are unique. The model presented here was capable of simulating the magnitude and phase of reflection coefficient reasonably well for three successive cycles and at two frequencies. The distribution curves were obtained from a rigorous iterative process by matching the simulated and measured reflection properties. It is important to point out that the pore solution distribution curves shown here resulted in good agreement between the simulated and measured reflection properties (magnitude and phase) at both frequencies. An earlier investigation conducted on a distilled water-soaked cube revealed that the temporal movement of the pore solution content peak and its widening (representing redistribution of pore solution) was crucial for the accurate simulation of the reflection properties. The resulting pore solution distribution curves also satisfy physical requirements such as diffusion and mass transport (i.e., evaporation, capillary draw, etc.) in cement-based materials. Also, there is no multiple scattering involved in the measurement process. Therefore, it is expected that the pore solution distribution obtained from this model very closely describe the actual pore solution distribution and its temporal variation in the cube. Finally, it is of utmost importance to note that the resulting pore solution distribution curves were capable of simulating the dip in the early days of the phase behavior at 3 GHz for all three cycles. Moreover, the argument that these curves might be unique is significantly strengthened by the fact that the same distribution functions also properly predicted the phase behavior at 10 GHz, which does not possess such a dip.

VIII. Conclusion

The results of a semiempirical model, simulating the microwave reflection properties of mortar exposed to cyclical soaking in salt solution and drying, at two distinct frequencies were presented. The model was initially developed to simulate the reflection properties of mortar exposed to water. The additional influences caused by salt solution ingress, including changes in pore solution concentration, volume, and distribution, as well as the formation of solid products due to salt solution ingress, were incorporated into the model.

The results showed good agreement between the measured and simulated reflection properties of the cube at both 3 GHz and 10 GHz. An important outcome of the model is the temporal pore solution distribution inside the mortar cube for the three successive soaking and drying cycles. The distribution functions that were employed followed a well-known behavior (Rayleigh-like). However, its specific parameters that determine the shape of the distribution for any day were determined empirically. The resulting pore solution distribution functions can be used to evaluate pore solution content at any depth in the mortar for any day of any cycle. Moreover, these distribution functions account for evaporation, increasing ionic concentration, and formation of solid products as well as movement of pore solution both toward the core and toward the surface of the cube. It is this fact that enabled the model to correctly simulate the dip in the phase of reflection coefficient at 3 GHz during the first few days of all three cycles.

The pore solution distributions for cycle 1 show that for the first few days of the cycle, the peak of the pore solution content decreases rapidly, indicating that most of the water that evaporates is from the near-surface layers of the cube. However, somewhat of a different behavior is observed for cycles 2 and 3. For these cycles, it is observed that during the first few days of the cycle, the peak does not drop as quickly. On the contrary, there is actually a *slight* increase in the peak pore solution content from day 2 to day 3 for cycle 2. However, there is a noticeable decrease in the pore solution content in the deeper layers (toward the core) for both the cycles, likely indicating that the pore solution is drawn from the core toward the surface after which it evaporates. Although this might seem like an anomaly, only a thorough investigation into this aspect would confirm which of the two processes i.e., whether the water that evaporates is mainly from the layers near the surface (as in the case of cycle 1) or if the water is drawn from the core to the surface after which it evaporates (as in the case of cycles 2 and 3) is the actual phenomena that occurs within the mortar cube. The results of such an investigation would then provide us with an overall insight into the mechanism of moisture movement/redistribution within the cubes and whether it is possible to have contrasting phenomena for different cycles. It is, however, believed that these contrasting phenomena, if true, could be as a result of the hygroscopic properties of the solid products (i.e.,

salt that has precipitated out of the pore solution) which become more pronounced as a function of cycles. This particular issue is currently the focus of an ongoing investigation. The difference between moisture distribution for the cases of water and saltwater, for cycle 2, also indicated the influence of salt as described above [42].

Finally, this model is very versatile so that it can take into account other phenomenon that may be occurring in the cube as well as easily accommodating any changes in the assumptions made here in addition to incorporating geometrical factors, etc.

REFERENCES

[1] "Cathodic protection of reinforced concrete bridge elements: A state-of-the-art report," ELTECH Research Corp., SHRP-S-337, 1993.

[2] "1991 Status of the Nation's Highways and Bridges: Conditions, Performance, and Capital Investment Requirements," Federal Highway Admin., Washington, DC, Jul. 2, 1991.

[3] G. P. Gu and J. J. Beaudoin, "Research on cost-effective solutions for corrosion prevention and repair in concrete structures," *Construction Canada*, vol. 39, no. 6, pp. 36–39, Nov./Dec. 1997.

[4] A. M. Neville, *Properties of concrete*, 4th ed. New York: Wiley, 1996, ch. 11.

[5] A. Rosenberg, C. M. Hansson, and C. Andrade, "Mechanisms of corrosion of steel in concrete," in *Materials Science of Corrosion I*. Westerville, OH: Amer. Ceramic Soc., 1989.

[6] J. Khanna, P. Seabrook, B. C. Gerwick, and J. Bickley, "Investigation of distress in precast concrete piles at Rodney Terminal," *Performance of Concrete in Marine Environment*, vol. ACI SP-109, pp. 277–320, 1988.

[7] O. E. Gjorv, "Steel corrosion in concrete structures exposed to norwegian environment," *Concrete Int.*, pp. 35–39, Apr. 1994.

[8] "Standard test methods for chemical analysis of hydraulic cement," in *Annual Book of ASTM Standards*. Philadelphia, PA: ASTM, 1995. ASTM C 114-95 04.01.

[9] "Methods of Sampling and Testing," Amer. Assoc. State Highway and Transportation Officials, Washington, DC, AASHTO T 260-82, 1986.

[10] "Standard test method for water-soluble chloride in mortar and concrete," in *Annual Book of ASTM Standards*. Philadelphia, PA: ASTM, 1995, vol. 04.01. ASTM C 1218-92.

[11] K. C. Clear and E. T. Harrigan, "Sampling and Testing for Chloride Ion in Concrete," Federal Highway Admin., Washington, DC, FHWA-RD-77-85, Aug. 1977.

[12] "Electrical Indication of Concrete's Ability to Resist Chlorides," Amer. Assoc. State Highway and Transportation Officials, Washington, DC, AASHTO T 277-93, 1993.

[13] "Electrical indication of concrete's ability to resist chloride ion penetration," in *Annual Book of ASTM Standards*. Philadelphia, PA: ASTM, 1995, vol. 04.01. ASTM C 1202-94.

[14] "Resistance of Concrete to Chloride Penetration," Amer. Assoc. State Highway and Transportation Officials, Washington, DC, AASHTO T 259-80, 1980.

[15] R. Zoughi, S. Gray, and P. S. Nowak, "Microwave nondestructive estimation of cement paste compressive strength," *ACI Mater. J.*, vol. 92, no. 1, pp. 64–70, Jan.–Feb. 1995.

[16] W. Shalaby and R. Zoughi, "Analysis of monopole sensors for cement paste compressive strength estimation," *Res. Nondestructive Eval.*, vol. 7, no. 2/3, pp. 101–105, 1995.

[17] K. Mubarak, K. J. Bois, and R. Zoughi, "A simple, robust and on-site microwave technique for determining water-to-cement (w/c) ratio of fresh portland cement-based materials," *IEEE Trans. Instrum. Meas.*, vol. 50, no. 5, pp. 1255–1263, Oct. 2001.

[18] K. Bois, R. Mirshahi, and R. Zoughi, "Dielectric mixing models for cement based materials," in *Proc. Review Progress Quantitative NDE*, vol. 16A, 1997, pp. 657–663.

[19] K. Bois, A. Benally, P. S. Nowak, and R. Zoughi, "Microwave nondestructive determination of sand to cement (s/c) ratio in mortar," *Res. Nondestructive Evaluation*, vol. 9, no. 4, pp. 227–238, 1997.

[20] A. Joisel, K. J. Bois, A. D. Benally, R. Zoughi, and J. C. Bolomey, "Embedded modulated dipole scattering for near-field microwave inspection of concrete: Preliminary investigation," *Proc. SPIE Subsurface Sensors Applications Conf.*, vol. 3752, pp. 208–214, Jul. 18–23, 1999.

[21] K. Bois, A. Benally, and R. Zoughi, "Microwave near-field reflection property analysis of concrete for material content determination," *IEEE Trans. Instrum. Meas.*, vol. 49, no. 1, pp. 49–55, Feb. 2000.

[22] K. J. Bois, A. D. Benally, P. S. Nowak, and R. Zoughi, "Cure-state monitoring and water-to-cement ratio determination of fresh portland cement based materials using near field microwave techniques," *IEEE Trans. Instrum. Meas.*, vol. 47, no. 3, pp. 628–637, Jun. 1998.

[23] K. Bois and R. Zoughi, "A decision process implementation for microwave near-field characterization of concrete constituent makeup," *Advances Applicat. Microw. Millimeter Wave Nondestructive Eval. (Special Issue Subsurface Sensing Technologies and Applications)*, vol. 2, no. 4, pp. 363–376, Oct. 2001.

[24] S. Kharkovsky, M. Akay, U. Hasar, and C. Atis, "Measurement and monitoring of microwave reflection and transmission properties of cement-based specimens," in *Proc. IEEE Instrumentation and Measurement Technology Conf.*, Budapest, Hungary, May 21–23, 2001, pp. 513–518.

[25] K. Bois, H. Campbell, A. Benally, P. S. Nowak, and R. Zoughi, "Microwave noninvasive detection of grout in masonry," *Masonry J.*, vol. 16, no. 1, pp. 49–54, Jun. 1998.

[26] D. Hughes, M. Kazemi, K. Marler, J. Myers, R. Zoughi, and T. Nanni, "Microwave detection of delamination between fiber reinforced polymer (FRP) composites and hardened cement paste," in *Proc. 28th Annu. Rev. Progress in Quantitative Nondestructive Evaluation*, vol. 21, Brunswick, ME, Jul. 29–Aug. 3 2001, pp. 512–519.

[27] J. Li and C. Liu, "Noncontact detection of air voids under glass epoxy jackets using a microwave system," *Advances Applicat. Microw. Millimeter Wave Nondestructive Eval. (Special Issue Subsurface Sensing Technologies and Applications)*, vol. 2, no. 4, pp. 411–423, Oct. 2001.

[28] K. Bois, A. Benally, and R. Zoughi, "Near-field microwave noninvasive determination of NaCl in mortar," in *Inst. Elect. Eng. Proc. Science, Measurement, Technology (Special Issue on Non-destructive Testing and Evaluation)*, vol. 148, Jul. 2001, pp. 178–182.

[29] C. Hu, A. Benally, T. Case, R. Zoughi, and K. Kurtis, "Influence on the near-field microwave reflection properties of chloride in mortar specimens made of cement types II, III, and V at X- and S-bands," in *Proc. SPIE Conf.*, vol. 4129, San Diego, CA, Jul. 30–Aug. 4 2000, pp. 31–38.

[30] C. Hu, T. Case, M. Castle, R. Zoughi, and K. Kurtis, "Microwave evaluation of accelerated chloride ingress in mortar," in *Proc. 27th Annu. Rev. Progress in Quantitative Nondestructive Evaluation*, vol. 20A, Ames, IA, Jul. 17–21, 2000, pp. 467–473.

[31] J. Case, R. Zoughi, K. Donnell, D. Hughes, and K. E. Kurtis, "Microwave analysis of mortar prepared with type I/II, III, and V cement and subjected to cyclical chloride exposure," in *Proc. 28th Annu. Rev. Progress in Quantitative Nondestructive Evaluation*, vol. 21, Brunswick, ME, Jul. 29–Aug. 3 2001, pp. 498–505.

[32] S. Peer, J. Case, K. Donnell, D. Hughes, R. Zoughi, and K. E. Kurtis, "Investigation of microwave reflection properties of mortar exposed to wet-dry cycles of tap water and chloride bath," in *Proc. 28th Annu. Rev. Progress in Quantitative Nondestructive Evaluation*, vol. 21, Brunswick, ME, Jul. 29–Aug. 3 2001, pp. 1269–1276.

[33] R. Zoughi, S. Peer, J. Case, E. Gallaher, and K. E. Kurtis, "Microwave near-field evaluation of the effects of cyclical chloride exposure and compressive loading on mortar," in *Proc. 3rd Int. Workshop Structural Health Monitoring (IWSHM)*. Stanford, CA, Sep. 12–14, 2001, pp. 575–583.

[34] S. Peer, J. T. Case, E. Gallaher, K. E. Kurtis, and R. Zoughi, "Microwave reflection and dielectric properties of mortar subjected to compression force and cyclically exposed to water and sodium chloride solution," *IEEE Trans. Instrum. Meas.*, vol. 52, no. 1, pp. 111–118, Feb. 2003.

[35] S. Peer, K. E. Kurtis, and R. Zoughi, "An electromagnetic model for evaluating temporal water content distribution and movement in cyclically soaked mortar," *IEEE Trans. Instrum. Meas.*, vol. 53, no. 2, pp. 406–415, Apr. 2004.

[36] F. T. Ulaby, R. K. Moore, and A. K. Fung, *Microwave Remote Sensing: Active and Passive*. Dedham, MA: Artech House, 1986, vol. 3, pp. 2017–2025.

[37] A. Sihvola, *Electromagnetic Mixing Formulas and Applications*. London, U.K.: Inst. Elect. Eng. Electromagnetic Series 47, 1999.

[38] S. Bakhtiari, S. Ganchev, N. Qaddoumi, and R. Zoughi, "Microwave noncontact examination of disbond and thickness variation in stratified composite media," *IEEE Trans. Microw. Theory Tech.*, vol. 42, no. 3, pp. 389–395, Mar. 1994.

[39] V. Kraszewski, *Microwave Auqametry*. Piscataway, NJ: IEEE Press, 1996, ch. 9.
[40] K. Hong and R. D. Hooton, "Effects of cyclic chloride exposure on penetration of concrete cover," *Cement and Concrete Res.*, vol. 29, pp. 1379–1386, 1999.
[41] S. Peer, "Nondestructive evaluation of moisture and chloride ingress in cement-based materials using near-field microwave techniques," M.S. thesis, Electrical and Computer Eng. Dept., Univ. Missouri-Rolla, Rolla, MO, Nov. 2002.
[42] S. Peer and R. Zoughi, "Comparison of water and saltwater movement in mortar based on a semi-empirical electromagnetic model," *IEEE Trans. Instrum. Meas.*, vol. 53, no. 4, pp. 1218–1223, Aug. 2004.

Shanup Peer received the B.Tech. degree in electrical and electronics from the University of Kerala, Kerala, India, in 1999 and the M.S. degree in electrical engineering from the University of Missouri, Rolla, in 2002.

From 2000 to 2002, he was a Graduate Research Assistant at the Applied Microwave Nondestructive Testing Laboratory (AMNTL), University of Missouri.

Kimberly (Kim) E. Kurtis received the B.S.E. degree in civil engineering *summa cum laude* from Tulane University, New Orleans, LA, in 1994 on a full-tuition Dean's Honor Scholarship and the M.S. and Ph.D. degrees from the University of California, Berkeley, in 1995 and 1998, respectively, under a Henry Hilp Fellowship and an NSF Graduate Fellowship.

She has been with the School of Civil and Environmental Engineering at the Georgia Institute of Technology (Georgia Tech), Atlanta, since January 1999, where she is currently an Associate Professor. Her research interests center on construction materials, with a strong emphasis on microstructure and durability of cement-based materials.

Dr. Kurtis is Chairman of the American Concrete Institute (ACI) Committee E802: Teaching Methods and Educational Materials, Secretary of ACI Committee 236: Materials Science of Concrete, and Associate Member of ACI Committee 201: Durability. She is Associate Editor for the *ASCE Journal of Materials in Civil Engineering* and is on the editorial board for *Cement Concrete Composites*. She received her School's Innovation Award (2002) and the Outstanding Undergraduate Research Mentor Award (2004), and was named ASCE's *Outstanding Faculty of the Year* (2003–2004) by the Georgia Tech student chapter.

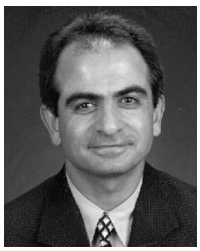

Reza Zoughi (S'85–M'86–SM'93) received the B.S.E.E., M.S.E.E., and Ph.D. degrees in electrical engineering (radar remote sensing, radar systems, and microwaves) from the University of Kansas, Lawrence.

From 1981 to 1987, he was with the Radar Systems and Remote Sensing Laboratory (RSL), University of Kansas. Currently, he is the Schlumberger Distinguished Professor of Electrical and Computer Engineering at the University of Missouri-Rolla (UMR). Prior to joining UMR in January 2001, and since 1987, he was with the Electrical and Computer Engineering Department at Colorado State University (CSU), Fort Collins, where he was a Professor and established the Applied Microwave Nondestructive Testing Laboratory (AMNTL). His current areas of research include developing new nondestructive techniques for microwave and millimeter wave inspection and testing of materials (NDT), developing new electromagnetic probes to measure characteristic properties of material at microwave frequencies, and developing embedded modulated scattering techniques for NDT purposes in particular for complex composite structures. He held the position of Business Challenge Endowed Professor of Electrical and Computer Engineering from 1995 to 1997 while at CSU. He has to his credit over 300 journal publications, conference proceedings and presentations, technical reports, and overview articles. He is also the author of a graduate textbook entitled "*Microwave Nondestructive Testing and Evaluation Principles*" (New York: Kluwer Academic, 2000) and the coauthor with A. Bahr, and N. Qaddoumi of a chapter on Microwave Techniques in an undergraduate introductory textbook entitled "*Nondestructive Evaluation: Theory, Techniques, and Applications*" edited by P. J. Shull (New York: Marcel Dekker, 2002). He has seven patents to his credit all in the field of microwave nondestructive testing and evaluation. He has given numerous invited talks on the subject of microwave nondestructive testing and evaluation.

Dr. Zoughi has received two Outstanding Teaching Commendations, an Outstanding Teaching Award, and the Dean of Engineering Excellence in Teaching Award since at UMR. He was voted the most outstanding teaching faculty seven times by the junior and senior students at the Electrical and Computer Engineering Department at CSU. He received the College of Engineering Abell Faculty Teaching Award in 1995. He is the 1996 recipient of the Colorado State Board of Agriculture Excellence in Undergraduate Teaching Award (only one faculty recognized for this award at each of the three CSU system campuses). He was recognized as an Honored Researcher for seven years by the Colorado State University Research Foundation. He is a Member of Sigma Xi, Eta Kappa Nu, and the American Society for Nondestructive Testing (ASNT). He is an Associate Technical Editor for the IEEE TRANSACTIONS ON INSTRUMENTATION AND MEASUREMENT, *Research in Nondestructive Evaluation* and *Materials Evaluation*, and served as the Guest Associate Editor for the Special Microwave NDE Issue of *Research in Nondestructive Evaluation*, and in 1995 and Co-guest Editor for the Special Issue of *Subsurface Sensing Technologies and Applications: Advances and Applications in Microwave and Millimeter Wave Nondestructive Evaluation*. He served as the Research Symposium Co-Chair for the American Society for Nondestructive Testing (ASNT) Spring Conference and 11th Annual Research Symposium in March 2002 in Portland, OR and as the Technical Chair for the IEEE Instrumentation and Measurement Technology Conference (IMTC2003) in May 2003 in Vail, CO. He served as the Guest Editor for the IMTC2003 special issue of the IEEE TRANSACTIONS ON INSTRUMENTATION AND MEASUREMENT. He is also a Member of the Administrative Committee (AdCom) of the IEEE Instrumentation and Measurement Society (2005–2008).